

DESIGN AND FIELD ANALYSIS OF A LARGE APERTURE QUADRUPOLE MAGNET

Kuanjun Fan[#], Koji Ishii, Susumu Igarashi, Takuya Sugimoto, Tatsunobu Shibata, Hiroshi Matsumoto
High energy accelerator research organization

Abstract

The J-PARC main ring fast extraction (FX) system provides bipolar magnetic field for both the abort beam at any energy and the FX beam at 30 GeV. With the increase of beam intensity, one great concern is the expected beam losses in the FX system region due to the restriction of the present quadrupole (QDT155) physical aperture. An upgrade study of design a new quadrupole with physical aperture 1.5 times larger is in process. The large physical aperture not only brings the problem of material saturation but also creates significant fringe fields that affect the particle motion. Since FX magnets at downstream are dense packed, magnetic field interference between the QDT155 and the septum has to be taken into consideration. This paper introduces the optimization of the quadrupole design, and how to treat the fringe field correctly for beam optics study.

1. Introduction

The fast extraction (FX) system of J-PARC main ring (MR) has two functions: extract normal beam at 30 GeV to the neutrino experimental target, and abort beam at any energy to the garbage when the interlock system is fired. In order to provide sufficient bending angle to the high rigidity FX beam, a group of kickers and septum magnets are employed. Fig. 1 shows the layout of the FX system, which occupies most of the third long straight section of the MR. Several quadrupole magnets are involved in the FX beam orbit, among which the QDT155 that located between the low field septa and the high-field septa plays an important role in FX beam operation. Since both the FX beam and the aborted beam have significant deviation from the beam axis before enter into the QDT155, they require the physical aperture of QDT155 must big enough to accommodate them without beam loss [1]. However, all FX elements are designed for high energy of 50 GeV operation in low beam intensity, which does not require large physical aperture. Now the maximum FX beam energy reduces from 50 GeV to 30 GeV, the beam size will increase that can “eat” the marginal space significantly of all FX elements particularly at the QDT155 due to the large off-axis of the extracted beam.

Now, the JPARC is being upgraded to increase its beam power to the design limit of 720 kW by increasing the beam intensity and the operation repetition rate, which will impose high requirements to the FX system. One great concern is the expected high intensity beam losses in the FX system region due to the restriction of physical aperture. Thus all the FX system septa have to be redesigned with enlarged physical aperture that can accommodate beam with emittance of $60 \pi \text{ mm.mrad}$.

Simulation shows the if the bore radius of the QDT155 increases from 75 mm to 110 mm, the physical aperture is big enough to accommodate high intensity beam without beam loss even if the beam is aborted at 3 GeV in the case of emergency. However, several technical problems arise from large aperture QDT. The first is the high excitation current because it is proportional to bore radius. Thus a large number of ampere-turns coil is needed, which requires a big installation space that increase the magnet size. The second is the magnetic saturation at the pole tip, which will be a big problem that may worsen the field quality severely. One possible solution is to increase the length of the QDT magnet to mitigate the requirement of gap field but keep the same integral of gradient. Since the maximum beam energy for the new FX system is limited as 30 GeV, all new septa are designed with compact size so that it creates sufficient space for the long new QDT magnet. Another problem arises from the new magnet is the large fringe field that might deteriorate the optics of the ring. This paper deals with the design of the new QDT and studies the large fringe field of the new QDT magnet effects on beam optics.

2. Present Quadrupole QDT155

The present QDT155 was originally designed for the extraction of high energy beam of 50 GeV with low beam intensity. However, in the future operation, the extracted beam energy reduces to 30 GeV, while the beam intensity will increase nearly double to realize the beam power of 720 kW. The extracted beam emittance is expected to increase a lot due to the space charge effects, which may exceed the extraction acceptance of the QDT155 magnet causing beam loss.

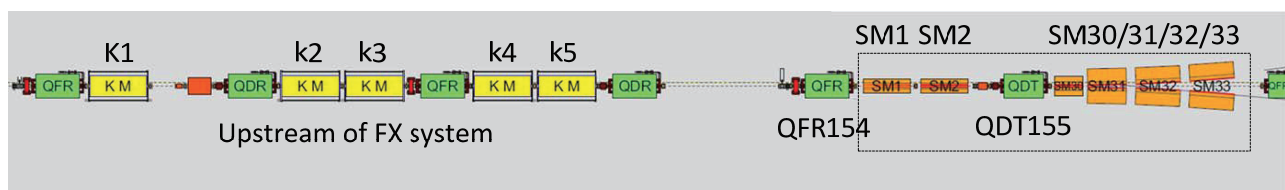


Figure 1: Layout of FX system.

[#] kj.fan@kek.jp

In order to examine the physical aperture of the QDT155, we have studied to track a realistic particle distribution through the 3D model. The x -values at the QDT155 exit is most critical to the operation since the extracted beam has its crest in the y -direction and could be lost due to a limited vertical aperture there. This can be seen from the Fig. 2, where the vertical apertures including the vacuum chamber thickness are plotted. It shows clearly that high intensity beam with 10π emittance will hit on pipe if the incident beam exits from the QFR154 (Fig. 1) with an initial angle of 0.55° . To avoid beam loss, the reference trajectory is preferred to closer to the QDT155 beam axis, which requires less kick angle from the low-field septa. However, it will impose higher demands of bending angle from downstream high-field septa, which creates difficulties for downstream high-field septa. To avoid such a difficulty, a large aperture QDT155 that can accommodate both high intensity extracted beam and abortion beam is being studied.

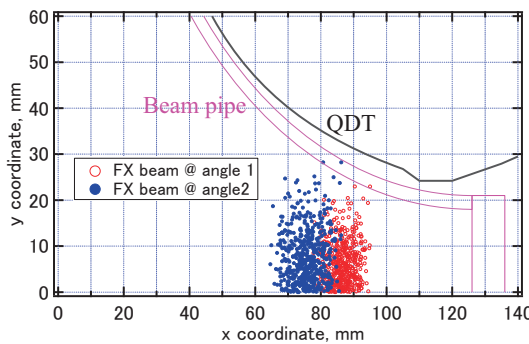


Figure 2: Limitation of QDT155 aperture.

3. Large aperture Q magnet design

In order to avoid too high field at pole tip causing magnetic saturation. The magnet length has to be increased 500 mm to reduce the required gap field, while maintain the same gradient integral. However, the lattice symmetry is broken if only one QDT155 is changed, which leads to beam loss. Beam optics study shows that three QDTs are needed at least to ensure beam quality. After optimization of the pole profile to avoid saturation, the cross section of the new large aperture QDT is shown in Fig. 3.

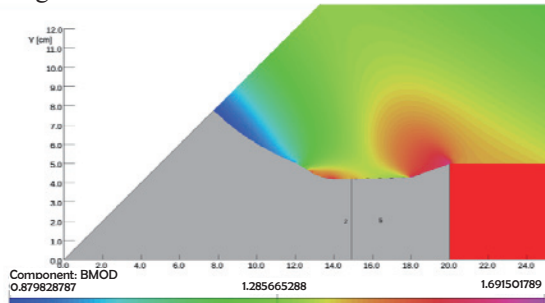


Figure 3: Field distribution in large aperture Q magnet.

Large aperture of QDT155 leads to significant fringe field that creates defect effects on beams: 1) for circulation beam, the fringe field generates a s -dependent focusing function $k(s)$ that may change the optics parameters, and 2) for extracted beam, the field along the extracted beam orbit may contain significant non-linear field components that will worsen the extracted beam quality. Thus, detail 3D study of QDT155 is critical for the upgrade of FX system.

4. Large aperture QDT effects

Using a longer QDT155 with different gradient $k(s)$ to replace the present one may introduce deviation in lattice optics [2,3,4]. In practice, the QDT155 and the high-field septum SM30 are mounted densely due to the restriction of installation space. Significant magnetic interference will have effects on optics also. This will create difficulties in beam matching that might leads to emittance growth and may even cause beam losses especially in high beam power operation. Thus detail 3D calculations of both type of QDT have to be studied to compare the linear optical properties and performance.

4.1 Linear transfer matrices of QDT155

Two 3D model of the present QDT155 and the new one are constructed in OPERA-3D. The s -dependent focusing function $k(s)$ of the QDT can be obtained by 3D multipole expansion of radial field B_r . Fig. 4 illustrates the principle: a cylinder with radius R_{ref} coaxial with the QDT axis is constructed to cover all fringe fields at both ends, the field components B_r are calculated around a circle (R_{ref}) at different s -position. Then B_r components are Fourier decomposed that will yield s -dependent harmonics at radius R_{ref} .



Figure 4: Multipole field components calculation.

At a given longitudinal position, the radial component B_r is expressed as,

$$B_r(r, \theta) = \sum_{n=1}^{\infty} C_n \left(\frac{r}{R_{ref}} \right)^{n-1} \sin[n(\theta - \alpha_n)] \quad (1)$$

Where C_m and α_m are the amplitude and phase angle of the $2n$ -pole component for the total field, R_{ref} is the reference radius.

The linear normalized focusing function $k(s)$ of the QDT155 is obtained,

$$k(s) = \frac{2C_2(s)}{B\rho}$$

Where C_2 is the linear gradient and $B\rho$ is the magnetic rigidity.

Fig. 5 compares the normalized focusing function of the present and new QDT155, which has different distribution but has the same gradient integral $\int k(s)ds$.

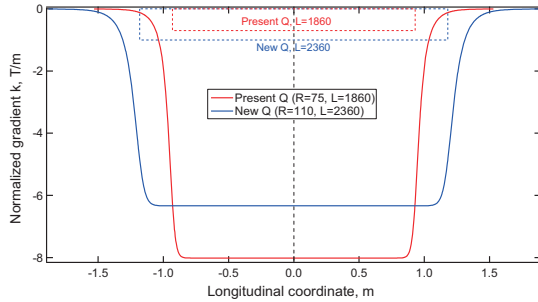


Figure 5: Focusing functions comparison.

The linear focusing function $k(s)$ of both different QDT models contain the all information of fringe field. The particle motion in a quadrupole is defined by second-order differential equations,

$$x'' - k(s)x = 0$$

$$y'' + k(s)y = 0$$

The ray traces and the transfer matrix elements can be obtained by numerical solving the differential equations [3]. Fig. 6 shows the matrix elements of the present QDT155 in x -direction.

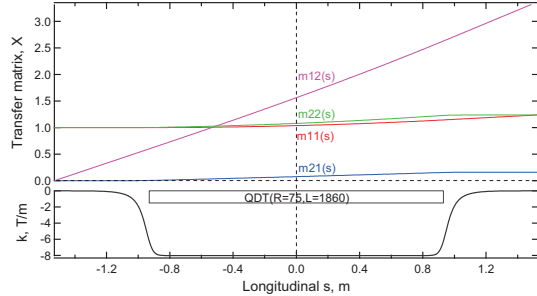


Figure 6: Matrix elements of present QDT155.

The transfer matrices $M_{x,p}$ and $M_{y,p}$ of the present defocusing QDT155 are evaluated as,

$$M_{x,p} = \begin{bmatrix} 1.2389 & 3.3704 \\ 0.1588 & 1.2389 \end{bmatrix} \quad M_{y,p} = \begin{bmatrix} 0.7765 & 2.7609 \\ -0.1439 & 0.7765 \end{bmatrix}$$

Since the QDT is symmetry, as a result, the diagonal of term in the matrices are equal and the determinants of the matrices are very close to unity.

The focusing length can be expressed simply as,

$$f_{x,y} = \frac{1}{m_{21}}$$

The present QDT focusing length in x and y direction are 6.3 mm and 6.95 m respectively. For the new QDT155, the four linear elements and ray traces in x -direction are plotted in Fig. 7.

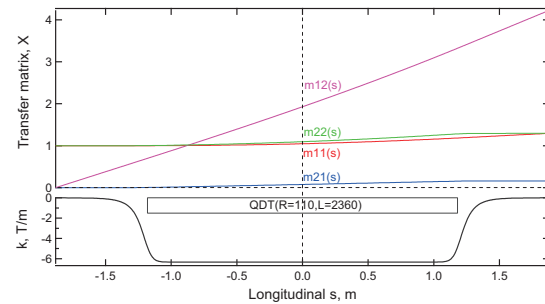


Figure 7: Matrix elements of new QDT155.

The resulting linear transfer matrices $M_{x,N}$ and $M_{y,N}$ of the new QDT in x and y direction are calculated,

$$M_{x,N} = \begin{bmatrix} 1.2961 & 4.2271 \\ 0.1609 & 1.2961 \end{bmatrix} \quad M_{y,N} = \begin{bmatrix} 0.7277 & 3.3172 \\ -0.1419 & 0.7277 \end{bmatrix}$$

The focusing length in x and y direction are 6.22 mm and 7.05 m respectively. These differences in optics parameters will worsen the matching condition, which needs further study.

4.2 Magnetic field interference

In reality, the QDT155 and the SM30 is close-packed in a limited space as shown in Fig. 8.

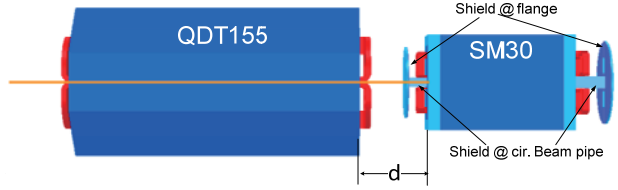


Figure 8: Magnetic field interference.

The magnetic field between these two magnets are overlapped, which leads to magnetic field interference. In the present case, there is no shield at the flange of SM30, which leads to significant magnetic interference. As shown in Fig. 9, the linear focusing function of the present QDT155 changes at downstream due to the presence of SM30.

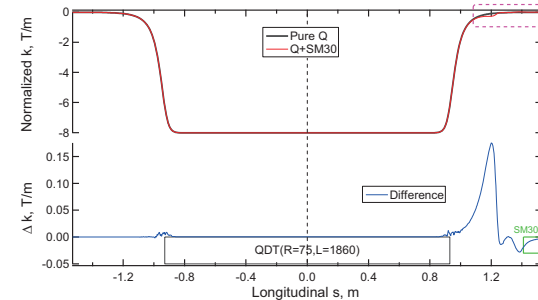


Figure 9: Present QDT155 $k(s)$ comparison W/O SM30.

To minimize the interference, shields are installed at the flange of new SM30, which results in significant reduction of magnetic interference as shown in Fig. 10.

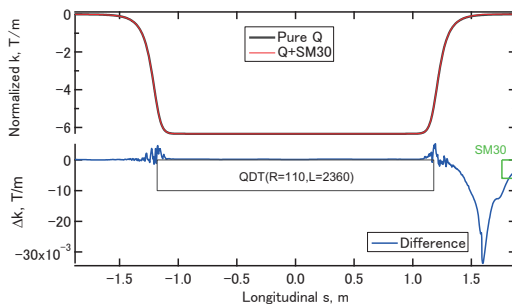


Figure 10: New QDT155 $k(s)$ comparison W/O SM30.

Compared with the designed value, the practical integrated gradient of QDT is changed because the field interference, which can be treated as a first-order perturbation. The equation of motion can be expressed by,

$$\begin{aligned}\delta x'' - k(s)\delta x &= \delta k(s)x \\ \delta y'' + k(s)\delta y &= -\delta k(s)y\end{aligned}$$

Where, $\delta k(s)$ is the perturbation error shown in Fig. 10. The total transfer matrix containing the effects of perturbation in the present assembly of QDT155 and SM30 can be obtained,

$$M_{x,Ep} = \begin{bmatrix} 1.2390 & 3.3707 \\ 0.1590 & 1.2494 \end{bmatrix} M_{y,Ep} = \begin{bmatrix} 0.7765 & 2.7607 \\ -0.1441 & 0.7761 \end{bmatrix}$$

The effects of perturbation δM_{err} is

$$\delta M_{err} = M_{x,P} - M_{x,EP}$$

In the same way, the practical transfer matrices of the new QDT and new SM30 assembly are,

$$M_{x,EN} = \begin{bmatrix} 1.2961 & 4.2271 \\ 0.1608 & 1.2959 \end{bmatrix} M_{y,EN} = \begin{bmatrix} 0.7277 & 3.3172 \\ -0.1419 & 0.7279 \end{bmatrix}$$

4.3 Magnetic field for extracted beam

The new QDT155 has large physical aperture that releases the restriction of bending angle provided by the upstream septa SM1 and SM2. Therefore we can make use of the capability of the new eddy current septa to generate as high as possible field to mitigate the demands on downstream high-field septa. So, the FX beam has large offset away from the beam axis and large angle before enter in to the assembly of QDT155 and SM30. When passing through the assembly, the FX beam will experience significant multipole field components, which can be deduced from 3D simulation as shown in Fig. 11.

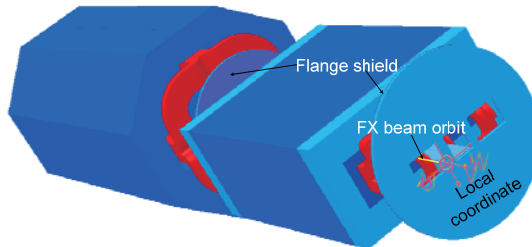


Figure 11: FX beam pass QDT and SM30 assembly.

The multipole field components can be obtained by 3D Fourier decomposition. First launch a proton particle with energy of 30 GeV at correct initial and position and angle, the orbit of the proton beam inside the assembly of QDT and SM30 can be obtained. A circular with reference R perpendicular to the orbit moves along the orbit, the radial field component B_r can be obtained and decomposed as has been explained in equation 1. Fig. 12 shows the field components seen by the FX beam, which contains dipole, quadrupole, sextupole and so on. The FX beam orbit and beam quality may be deteriorated by these fields. Further studies are need to predict the beam behaviour exactly.

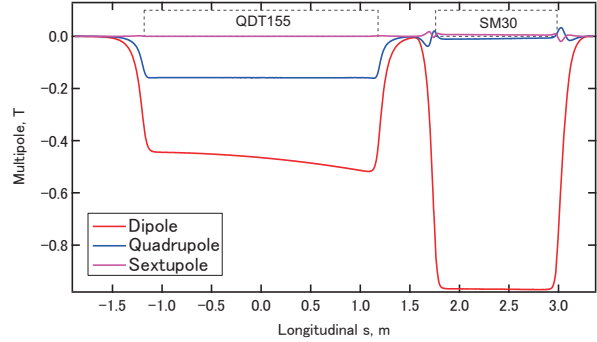


Figure 12: Multipole field seen by FX beam.

5. Summary

There is a defocus quadrupole QDT155 in the present FX system of J-PARC main ring, which has the risk of beam loss in high beam power operation due to its insufficient physical aperture. A large aperture QDT is being studied to replace the present one. However, the new QDT may create mismatching in lattice optics due to the different s -dependent focusing function. The large fringe field between the assembly of QDT and SM30 may result in magnetic interference to deviate the optics matching further. Measures need to be taken to eliminate these defects.

Reference

- [1] K. Fan, et al., "Upgrade of J-PARC fast extraction system", Proceedings of the IPAC2014, Dresden, Germany, June 15-20, 2014
- [2] G.E. Lee-whiting, Nucl. Instrum. Methids. 76 305, 1969.
- [3] J.G. Wang, Phys. Rev. Spec. Top. -Acc. & Beams, 9, 122401, 2006.
- [4] J.G. Wang, Nucl. Instr. Meth. In Phy. Res. A, 648 (2011) 41-45.